Article

Current Biology

Metabolic dissimilarity determines the establishment of cross-feeding interactions in bacteria

Graphical abstract

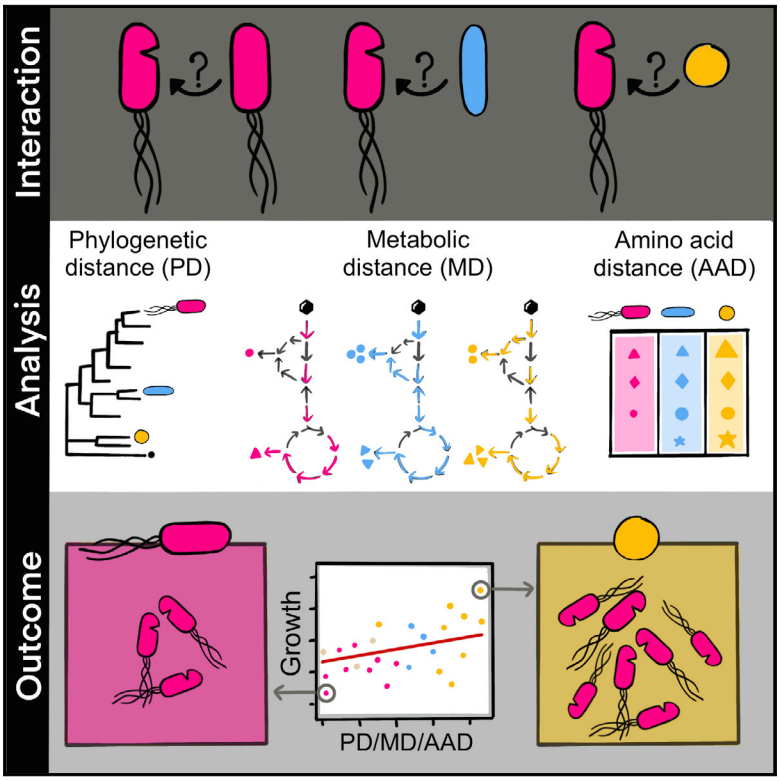

Authors

Samir Giri, Leonardo Oña, Silvio Waschina, Shraddha Shitut, Ghada Yousif, Christoph Kaleta, Christian Kost

Correspondence

samirgiri2809@gmail.com (S.G.), christiankost@gmail.com (C.K.)

In brief

Giri et al. study the factors that determine the establishment of obligate unidirectional cross-feeding between two bacterial populations. Combining experiments with *in silico* simulations of a gut bacterial community, the authors show that metabolic interactions are more likely to establish between unrelated and metabolically dissimilar genotypes.

Highlights

- Auxotrophic and prototrophic bacteria readily engaged in metabolic cross-feeding
- Recipient growth correlated with phylogenetic and metabolic distance to donors
- Cross-feeding is more likely to establish between metabolically dissimilar strains

Giri et al., 2021, Current Biology *31*, 5547–5557
December 20, 2021
https://doi.org/10.1016/j.cub.2021.10.019

CellPress

Current Biology

CellPress

Article

Metabolic dissimilarity determines the establishment of cross-feeding interactions in bacteria

Samir Giri,[1,2,*] Leonardo Oña,[2] Silvio Waschina,[3,4] Shraddha Shitut,[1,2,6] Ghada Yousif,[1,2,5] Christoph Kaleta,[4] and Christian Kost[1,2,7,*]

[1]Experimental Ecology and Evolution Research Group, Department of Bioorganic Chemistry, Max Planck Institute for Chemical Ecology, 07745 Jena, Germany

[2]Department of Ecology, School of Biology/Chemistry, University of Osnabrück, 49076 Osnabrück, Germany

[3]Institute for Human Nutrition and Food Science, Nutriinformatics, Christian-Albrechts-University Kiel, 24105 Kiel, Germany

[4]Research Group Medical Systems Biology, Institute for Experimental Medicine, Christian-Albrechts-University Kiel, 24105 Kiel, Germany

[5]Department of Botany and Microbiology, Faculty of Science, Beni-Suef University, Beni-Suef, Egypt

[6]Present address: Institute of Biology, University of Leiden, 2333 Leiden, the Netherlands

[7]Lead contact

*Correspondence: samirgiri2809@gmail.com (S.G.), christiankost@gmail.com (C.K.)

https://doi.org/10.1016/j.cub.2021.10.019

SUMMARY

The exchange of metabolites among different bacterial genotypes profoundly impacts the structure and function of microbial communities. However, the factors governing the establishment of these cross-feeding interactions remain poorly understood. While shared physiological features may facilitate interactions among more closely related individuals, a lower relatedness should reduce competition and thus increase the potential for synergistic interactions. Here, we investigate how the relationship between a metabolite donor and recipient affects the propensity of strains to engage in unidirectional cross-feeding interactions. For this, we performed pairwise cocultivation experiments between four auxotrophic recipients and 25 species of potential amino acid donors. Auxotrophic recipients grew in the vast majority of pairs tested (63%), suggesting metabolic cross-feeding interactions are readily established. Strikingly, both the phylogenetic distance between donor and recipient and the dissimilarity of their metabolic networks were positively associated with the growth of auxotrophic recipients. Analyzing the co-growth of species from a gut microbial community *in silico* also revealed that recipient genotypes benefitted more from interacting with metabolically dissimilar partners, thus corroborating the empirical results. Together, our work identifies the metabolic dissimilarity between bacterial genotypes as a key factor determining the establishment of metabolic cross-feeding interactions in microbial communities.

INTRODUCTION

Microorganisms are ubiquitous on our planet and are key for driving pivotal ecosystem processes.[1–3] They contribute significantly to the flow of elements in global biogeochemical cycles[3,4] and are also crucial for determining the fitness of plants[5,6] and animals,[7,8] including humans.[9,10] These vital functions are provided by complex communities that frequently consist of hundreds or even thousands of metabolically diverse strains and species.[11,12] However, the rules that determine the assembly, function, and evolution of these microbial communities remain unclear. Understanding the underlying governing principles is central to microbial ecology and crucial for designing microbial consortia for biotechnological[13] or medical applications.[14,15]

In recent years, both empirical and theoretical work has increasingly suggested that the exchange of essential metabolites among different bacterial genotypes is a crucial process that can significantly affect growth,[16,17] composition,[18] and the structure of microbial communities.[19] In these cases, one bacterial genotype releases a molecule into the extracellular environment, which other cells in the local vicinity can use. The released substances frequently include building-block metabolites, such as amino acids,[20,21] vitamins,[22,23] or nucleotides,[24] as well as degradation products of complex polymers.[19,25] Even though these compounds represent valuable nutritional resources, they are released as unavoidable byproducts of bacterial physiology[26,27] and metabolism[28] or due to leakage through the bacterial membrane.[29,30] Consequently, the released compounds create a pool of resources that can benefit members of the same or different species that are present in the same environment.[31–34] The beneficiaries include metabolically autonomous genotypes (i.e., prototrophs) that opportunistically take advantage of these metabolites as well as strains, whose survival essentially depends on an external supply with the corresponding metabolite (i.e., auxotrophs). Due to a mutation in their genome, these auxotrophic genotypes are unable to autonomously synthesize vital nutrients, such as amino acids, vitamins, or nucleotides. By utilizing metabolites that are produced by

another cell, a unidirectional cross-feeding interaction is established. Auxotrophic mutants that use compounds released by others can gain a significant fitness advantage over prototrophic cells that produce the required metabolites by themselves.[35] In addition, when co-occurring with strains that can provide the required metabolite, auxotrophic genotypes are commonly stabilized by negative frequency-dependent selection, which maintains their populations in the long run.[36–39] As a consequence of the strong fitness benefits that can result for auxotrophic genotypes as well as the stabilizing effect of negative frequency-dependent selection, cross-feeding between prototrophic donors and auxotrophic recipients is prevalent in all kinds of microbial ecosystems, including soil,[40] fermented food,[21] aquatic environments,[41,42] as well as host-associated microbiota.[7,43] Despite the ubiquity of unidirectional cross-feeding interactions in nature, the factors determining their establishment remain poorly understood.[44–47] In particular, it is unclear how the relationship between the metabolite donor and the auxotrophic recipient affects the likelihood that a cross-feeding interaction is successfully established. Two possibilities are conceivable.

First, phylogenetically closely related individuals are more likely to share physiological features that favor the establishment of cross-feeding interactions than two more distantly related strains. For example, an efficient transfer of metabolites from one cell to another commonly depends on close physical contact between donor and recipient.[48] The attachment to other cells is generally mediated by surface factors (e.g., adhesive proteins) or exopolymers that, in some cases, operate more effectively between cells sharing similar surface structures.[49] Moreover, some species form intercellular nanotubes to exchange metabolites between cells,[36,48] which in turn might require an increased structural similarity between cells for an efficient transport to operate. Another context, in which the phylogenetic relatedness between donor and recipient could determine the establishment of a unidirectional cross-feeding interaction, is when both partners can communicate with each other. Certain signals involved in chemical communication (i.e., quorum sensing) between cells are more readily perceived by more closely related bacterial strains than more distantly related individuals.[50] Consequently, quorum sensing between more similar genotypes is also more likely to regulate processes such as cell-cell adhesion[16] or the establishment of metabolic cross-feeding interactions.[51] In the following, we refer to this possibility as the similarity hypothesis.

Second, unidirectional cross-feeding interactions might be more likely to emerge among two more distantly related individuals than between two close relatives. For instance, two distantly related bacterial cells are less likely to share ecological preferences, such as habitat or resources utilized, than two phylogenetically similar bacterial taxa.[45,52,53] Consequently, two more distantly related strains should compete less for the available resources than two individuals that belong to the same or two closely related species.[54] Moreover, two phylogenetically distantly related cells will tend to have a more dissimilar metabolic network than two closely related individuals.[33,55,56] As a result, both the biosynthetic cost to produce a given metabolite and its nutritional value are more likely to differ in interspecific pairs than among members of the same species.[57,58] If these differences also translate into an enhanced growth of the auxotrophic recipient, a positive correlation between the growth of the auxotroph and the phylogenetic and/or metabolic distance to the donor cell would be observed. In the following, we refer to this alternative possibility as the dissimilarity hypothesis.

Here, we aim to distinguish between these two hypotheses to better understand the factors governing the establishment of this ecologically important interaction. To achieve this goal, we use unidirectional cross-feeding interactions as a model. Synthetically assembling pairs consisting of an auxotrophic recipient and a prototrophic amino acid donor of the same or a different species ensured that both interaction partners do not share a coevolutionary history. In this way, all results will represent the situation of a naive encounter between both interaction partners and only mirror effects resulting from the phylogenetic relatedness and metabolic dissimilarity between partners. Using this synthetic ecological approach, we systematically determined whether and how the phylogenetic or metabolic distance between auxotrophic recipients and prototrophic amino acid donors affects cross-feeding in pairwise bacterial consortia.

Our results show that, in the vast majority of cases tested, unidirectional cross-feeding interactions successfully established between a prototrophic donor and an auxotrophic recipient. Strikingly, recipients' growth was positively associated with both the phylogenetic and metabolic distance between donor and recipient. This pattern could partly be explained by the difference in the amino acid profiles produced by donors. Finally, analyzing the co-growth of species from a gut microbial community *in silico* revealed that recipient genotypes benefitted more from interacting with metabolically dissimilar partners, thus corroborating the empirical results. Together, our work identifies the metabolic dissimilarity between donor and recipient genotypes as a critical parameter determining the establishment of unidirectional cross-feeding interactions in microbial communities.

RESULTS

Auxotrophic recipients commonly benefit from the presence of prototrophic donor cells

To determine the probability with which unidirectional cross-feeding interactions emerge between an auxotrophic recipient and a prototrophic donor genotype, pairwise coculture experiments were performed (Figure 1A). For this, 25 strains that belonged to 21 different bacterial species were used as potential amino acid donors (Figures 1B and 1C). Donor strains were selected such that they represented different bacterial taxa and were able to synthesize all nutrients they required for growth in a minimal medium (metabolic autonomy and prototrophy; Figure 1C). In addition, none of the strains used were isolated from the same environment (key resources table), thus minimizing the possibility of a shared coevolutionary history. These potential amino acid donors were individually cocultured together with each of four auxotrophic recipients that belonged to one of two bacterial species (i.e., *Escherichia coli* and *Acinetobacter baylyi*) and were auxotrophic for either histidine (Δ*hisD*) or tryptophan (Δ*trpB*; Figure 1D).

To test whether the selected donor strains can support the growth of auxotrophic recipients, the abovementioned strains were systematically cocultured in all possible pairwise combinations (initial ratio: 1:1). Subsequently, the growth of the recipient

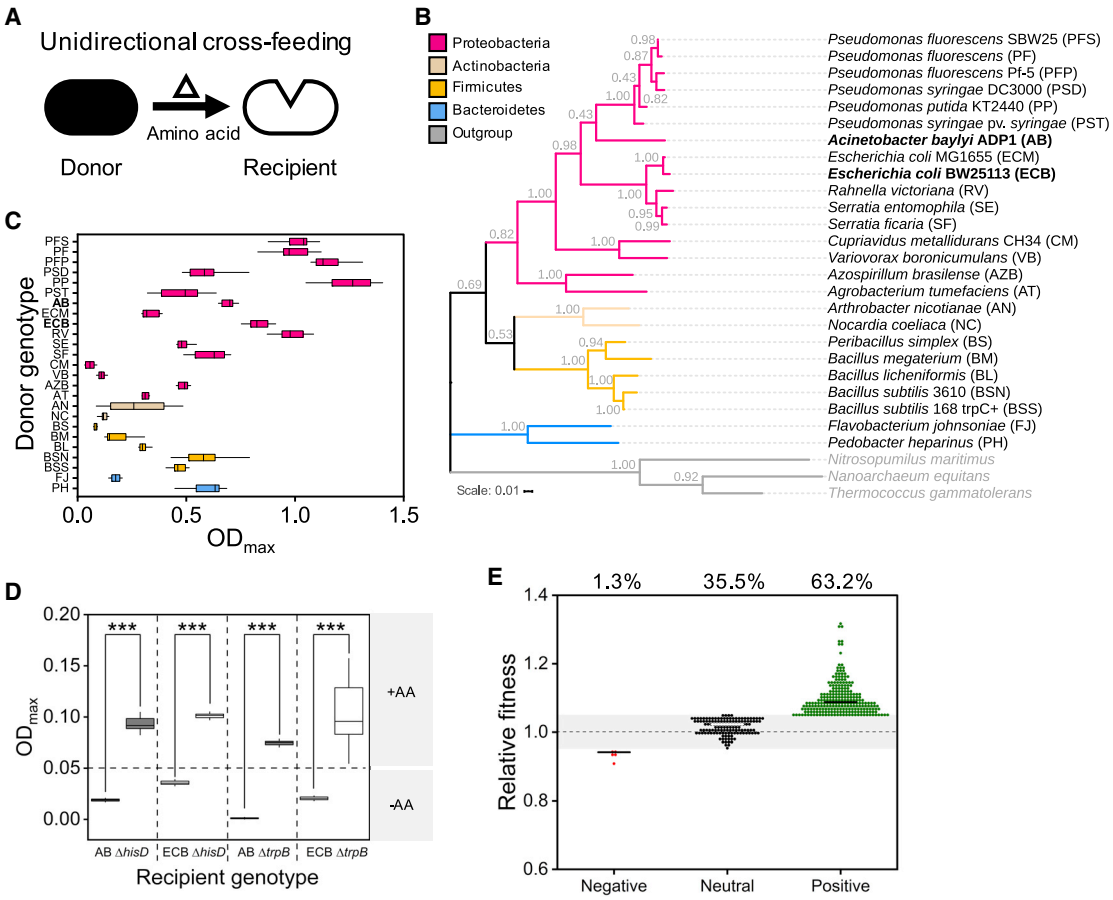

Figure 1. Unidirectional cross-feeding between prototrophic donor cells and amino acid auxotrophic recipients is common

(A) Overview over the experimental system used. Metabolically autonomous donor genotypes (black cell) were individually cultivated together with an auxotrophic recipient that was unable to produce either histidine or tryptophan (white cell). Growth of auxotrophs signifies the successful establishment of a unidirectional cross-feeding interaction, in which the focal amino acid (i.e., histidine or tryptophan [Δ]) is exchanged between donor and recipient cells.

(B) Phylogenetic tree of bacterial species (donors and recipients) used in this study. Different colors indicate different phyla. The tree was constructed based on the 16S rRNA gene. Species used as recipients are highlighted in bold. Branch node numbers represent bootstrap support values.

(C) Boxplot shows growth of 25 donor strains in minimal medium (n = 8). Donor genotypes were arranged based on their order in the phylogenetic tree, and colors correspond to different phyla (B). Recipient strains used in this study are highlighted in bold.

(D) Growth of recipient strains (*Acinetobacter* baylyi [AB] and *Escherichia coli* [ECB]) auxotrophic for histidine (Δ*hisD*) or tryptophan (Δ*trpB*), which have been cultivated in the presence (+AA) of the focal amino acid (100 μM) or without amino acid supplementation (−AA). Asterisks indicate the results of a paired sample t test: ***$p < 0.001$; n = 4. In both cases (C and D), growth was determined spectrophotometrically (optical density 600 nm [OD_{600nm}]). Boxplots: medians (lines within boxes), interquartile range (boxes), and 1.5× interquartile range (whiskers) are shown.

(E) Growth of auxotrophic recipients in pairwise coculture with different donor genotypes. *Escherichia coli* and *Acinetobacter* baylyi, each either auxotrophic for histidine (Δ*hisD*) or tryptophan (Δ*trpB*), were used as amino acid recipients. The relative fitness of receivers, when grown in coculture with one of 25 donors, is plotted relative to their growth in monoculture in the absence of the focal amino acid (gray dashed line).

Gray shaded area shows the threshold above (±1.05) and below (±0.95) which recipients have a fitness advantage and disadvantage, respectively, in coculture with the donor. Depending on whether the recipient's fitness was above or below the critical threshold, interactions were classified as negative (n = 5), neutral (n = 135), or positive (n = 240). CFU was calculated 24 h post-inoculation.

strains in coculture was quantified by determining the number of colony-forming units (CFUs) at the onset of the experiment (0 h) and after 24 h. The difference between both numbers was then compared to the growth, the same strain achieved in a monoculture over the same period without externally supplied amino acids. In this experiment, the donor's presence affected the recipient's growth either positively, negatively, or in a neutral way. Only 1.3% of tested cases showed a growth reduction, and in 35% of interactions, auxotrophs did not respond at all to the presence of a donor cell (Figure 1E). In contrast, in the vast majority of cocultures tested (i.e., 63.2%), the growth of auxotrophic cells was significantly enhanced in the presence of donor cells as compared to their growth in monocultures, suggesting that unidirectional cross-feeding interactions readily establish (Figure 1E).

Recipient growth depends on amino acid production of donor genotypes

The main factor causing growth of auxotrophs in the coculture experiment was likely the amount and identity of metabolites

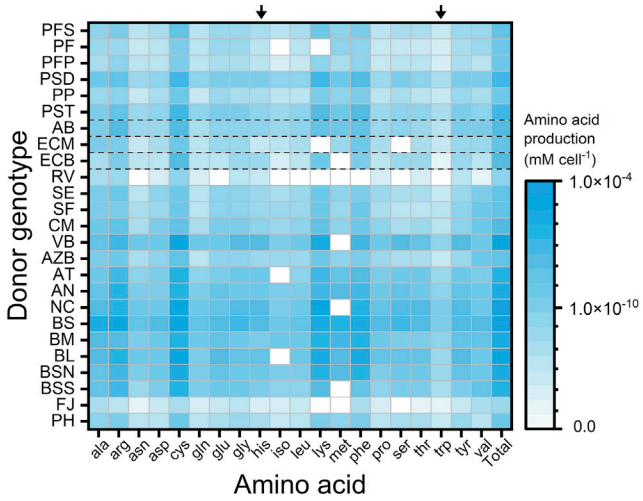

Figure 2. Amino acid production profile of different donors

Heatmap of amino acids released by different donor strains. The amount of amino acid (mM per cell) produced by 25 donor strains (for abbreviations, see Figure 1B) is shown (y axis). Cell-free supernatants of exponentially growing cultures were analyzed via LC-MS/MS. Colors indicate different amino acid concentrations (legend) and the total amount of amino acids produced by the donor. Arrows highlight the two focal amino acids used in the experiments (i.e., His and Trp). Mean values of four biological replicates are shown (see also Figures S1 and S2).

donor cells released into the extracellular environment (i.e., the exo-metabolome).[26] To test whether amino acid production of donors could explain the observed recipient growth, the supernatant of monocultures of all 25 donor strains was collected during exponential growth. Subjecting the cell-free supernatant of these cultures to liquid chromatography-tandem mass spectrometry (LC-MS/MS) analysis revealed that all tested genotypes secreted amino acids in varying amounts (Figures 2 and S1). In this experiment, donors are not expected to specifically produce the amino acid that the cocultured auxotroph requires for growth. Moreover, bacteria usually use generic transporters to import chemically similar amino acids.[59–61] Thus, auxotrophic recipients may benefit not only from the one amino acid they require for growth but potentially also from utilizing other amino acids that are produced by the donor. To quantitatively determine whether the released amino acids could explain the observed growth of recipients, the cell-free supernatant of donor cultures (replenished with fresh nutrients; STAR Methods) was supplied to monocultures of auxotrophic cells and the resulting growth over 24 h was quantified by plating. As expected, growth of auxotrophic recipients was positively associated with the concentration of the amino acid the corresponding auxotroph required for growth (Table 1; Figure S2A). Interestingly, however, was the observation that recipient growth also correlated positively with the total amount of amino acids present in the donor supernatant (Figure S2B). Notable in this context was the observation that the growth of the tryptophan-auxotrophic *Acinetobacter baylyi* (Δ*trpB*) strain was not positively associated with either the amount of tryptophan produced by donor genotypes or the total amount of amino acids they had produced. Given that both the concentration of the focal amino acid (FAA) and

Table 1. Total amino acid production of different donors can predict unidirectional cross-feeding

Recipient	n	ρ	p value
Total amino acids			
AB-his	89	0.29	4.3 × 10^{-3}[a]
AB-trp	90	0.17	0.12
ECB-his	92	0.35	8.3 × 10^{-4}[a]
ECB-trp	93	0.33	1.2 × 10^{-3}[a]
Focal amino acids			
AB-his	89	0.23	0.029[a]
AB-trp	90	0.09	0.37
ECB-his	92	0.47	0.2 × 10^{-5}[a]
ECB-trp	93	0.43	0.13 × 10^{-4}[a]

Overview of the statistical relationships between the effect of total amount of amino acids or the focal amino acids on the density auxotrophic recipients reached when supplied with the supernatant of different donor cultures. Density of auxotrophs was normalized by donor cell density. Results of Spearman rank correlations are shown (see also Figure S2).

[a]Significant effects ($p \leq 0.05$)

the total amount of amino acid (TAA) produced by donor genotypes could explain the growth of three out of four auxotrophs tested, we statistically removed the effect of the focal amino acid and reanalyzed the impact of the total amount of amino acids on recipient growth. This was achieved by first obtaining the residuals of a linear regression between TAA and FAA (i.e., the variation unexplained by total amino acid concentration). We then performed a new linear regression between these residuals and the growth of recipients. The results of this analysis revealed a significant correlation of both parameters for *E. coli* ($p < 0.05$), but not *A. baylyi* ($p > 0.05$; Table 1), thus indicating that *E. coli* auxotrophs likely also took advantage of other amino acids that were produced by the corresponding donors. This observation points to species-specific differences in the metabolic requirements of auxotrophic genotypes and shows that auxotrophic recipients can also take advantage of other (non-focal) amino acids that are produced by donor cells.

Recipient growth correlates positively with amino acid profile dissimilarity

To distinguish between the two main hypotheses, we asked whether the difference in the amino acid profile (i.e., the collection of secreted amino acids) produced by a closely and distantly related donor strain could explain the growth auxotrophs achieved in the coculture experiment. To test this, we calculated the Euclidean distance between the amino acid profiles of all 25 donor strains. Comparing the statistical relationship between the normalized growth of auxotrophs in coculture with the Euclidean distance in the amino acid profiles of closely and distantly related donor genotypes revealed a significantly positive relationship between both parameters in all four auxotrophs tested (Figure 3A). In other words, auxotrophs grew better in coculture with a donor, which produced an amino acid mixture, whose composition was different to the one a closely related cell would have produced. Thus, these results support the dissimilarity hypothesis.

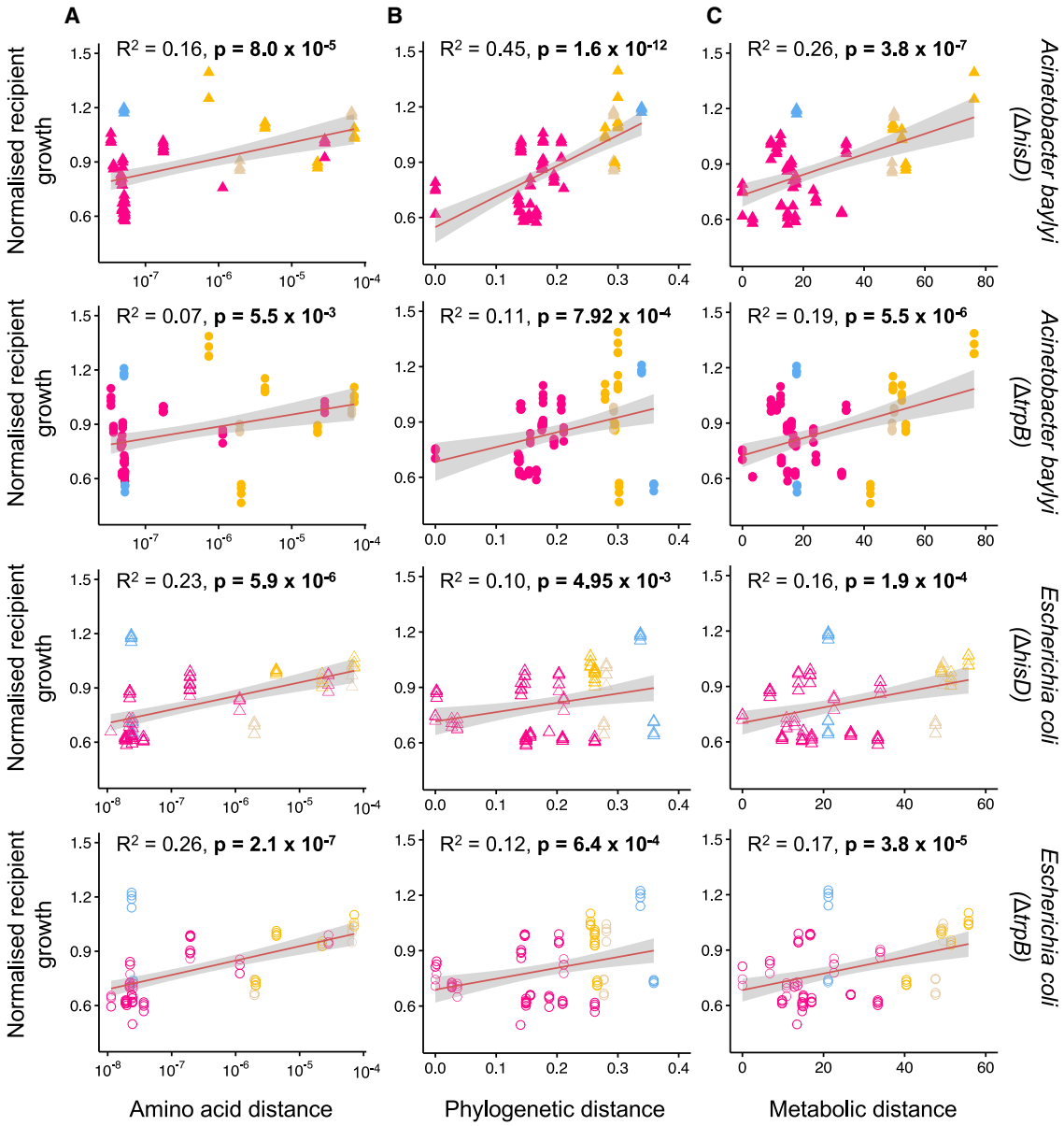

Figure 3. Cross-feeding increases with an increasing dissimilarity to donor cells

Shown is the net growth of the *E. coli* and *A. baylyi* recipients auxotrophic for histidine (Δ*hisD*; △) and tryptophan (Δ*trpB*; ○) as a function of (A) the amino acid profile distance, (B) the phylogenetic distance, and (C) the genome-based metabolic distance between donor and recipient. Red lines are fitted linear regressions, and gray areas indicate the 95% confidence interval. Each data point represents a replicate and is color-coded according to its phylogenetic affiliation (Figure 1B). Growth of recipients is displayed as the logarithm of the difference in the number of CFUs between 0 h and 24 h and was normalized per number of donor cells. Results of linear regression are shown, and significant results are highlighted in bold. Sample size was 80–100 in all cases.

Growth of recipients scales positively with the phylogenetic and metabolic distance to donor cells

Next, we asked whether two phylogenetically closely related genotypes are more likely to engage in a unidirectional cross-feeding interaction than two more distant relatives. To test this, we reanalyzed the results of the coculture experiment by focusing on the phylogenetic relatedness between donor and recipient genotypes. In this context, only those cocultures were considered in which auxotrophs showed detectable growth. These analyses revealed a positive association between the recipients' growth and its phylogenetic distance to donor cells (Figure 3B).

However, given that previous analyses suggested that differences in the amino acid profiles could predict the growth of auxotrophic recipients (Figure 3A), we reasoned that the phylogenetic distance might only approximate the difference in the strains' metabolic networks. To verify this, we additionally compared the genome-scale metabolic networks of all donor

Table 2. Corrected regression analysis of the effect of amino acid profile distance (AAD), phylogenetic distance (PD), and metabolic distance (MD) on recipient growth

Recipient	n	R^2	p value	R^2	p value	R^2	p value
		AAD corrected for PD				**MD corrected for PD**	
AB-his	87	0.02	0.2			0.003	0.59
AB-trp	100	0.04	0.06			0.09	3×10^{-3}[a]
ECB-his	80	0.17	0.013[a]			0.08	0.01[a]
ECB-trp	91	0.19	1.4×10^{-5}[a]			0.07	0.011[a]
		corrected for TAA		**PD corrected for TAA**		**MD corrected for TAA**	
AB-his	87	0.12	9.3×10^{-4}[a]	0.37	3.6×10^{-10}[a]	0.19	2.1×10^{-5}[a]
AB-trp	100	0.2	4.2×10^{-6}[a]	0.19	5.6×10^{-6}[a]	1.25	1.0×10^{-7}[a]
ECB-his	80	0.17	1.4×10^{-4}[a]	0.04	0.06	0.1	0.0047[a]
ECB-trp	91	0.24	7.2×10^{-7}[a]	0.085	0.005[a]	0.13	0.00042[a]
		AAD corrected for FAA		**PD corrected for FAA**		**MD corrected for FAA**	
AB-his	87	0.039	0.065	0.33	6.8×10^{-9}[a]	0.16	8.5×10^{-5}[a]
AB-trp	100	0.05	0.02[a]	0.08	4.3×10^{-3}[a]	0.15	5.8×10^{-5}[a]
ECB-his	80	0.06	0.02[a]	0.045	0.059	0.059	0.03[a]
ECB-trp	91	0.11	1.5×10^{-3}[a]	0.06	0.02[a]	0.06	0.02[a]

To disentangle the effect of individual parameters on the growth of auxotrophic recipients of *Acinetobacter baylyi* (AB) and *E. coli* (ECB), a linear regression for both MD and AAD was calculated with PD as the independent variable. In subsequent regressions, the residuals (i.e., variation not explained by PD) were used as independent variables.

To correct the effect that total amino acid (TAA) would have on the ability of AAD, PD, and MD to predict the growth of auxotrophic recipients, we first calculated a linear regression for AAD, PD, and MD with TAA as the independent variable. In subsequent regressions, the residuals (i.e., variation not explained by TAA) were then used as independent variables.

To correct the effect the focal amino acid (FAA) would have on the ability of AAD, PD, and MD to explain the growth of auxotrophic recipients, we first calculated a linear regression for AAD, PD, and MD with FAA as the independent variable. In subsequent regressions the residuals (i.e., variation not explained by FAA) were then used as independent variables.

See also Figure S3.

[a]Significant effects ($p \leq 0.05$)

genotypes. A metabolic similarity matrix between donor and recipient strains was calculated by identifying similarities and differences in both partners' biosynthetic pathways (hereafter: metabolic distance). Correlating the resulting data with the growth of auxotrophic recipients in coculture revealed a positive association between the metabolic distance and recipient growth (Figure 3C). Together, these results provide additional support for the hypothesis that cross-feeding interactions are more likely to establish between two more dissimilar genotypes.

All three distance measures alone can explain recipient growth

The observation that each of the three distance metrics analyzed (i.e., amino acid profile distance [AAD], phylogenetic distance [PD], and metabolic distance [MD]; Figure 3) correlated positively with recipient growth, yet none of the regression models of each parameter alone could explain all of the variation observed in recipient growth ($R^2 \leq 0.45$; Figure 3), suggested that all three factors operate simultaneously to cause the observed growth pattern. Hence, we asked whether any of these factors alone was sufficient to independently predict the growth of auxotrophic recipients. This question was addressed by replotting the data of the performed coculture experiments in three-dimensional graphs that display the growth of a given auxotroph, depending on two of the three measures quantified. Fitting a 2D plane into the resulting graphs indicated that increasing each of the three measures also increased recipients' growth (Figure S3). Thus, these graphs suggested that the three explanatory variables are likely correlated with each other. To subject this conjecture to a formal statistical test, we repeated the regression analyses to examine whether MD or AAD was significantly associated with the auxotrophs' growth in coculture when the first predictor variable, PD, was already included (Table 2). We first controlled for phylogeny because two more closely related species are genetically more similar and are thus also more likely to share certain traits and biochemical capabilities. In the majority of cases, the growth of *E. coli* recipients remained positively associated with metabolic distance as well as the distance of the amino acid production profile ($p < 0.01$; Table 2). However, the tryptophan auxotrophic *A. baylyi* strain (Δ*trpB*) showed only marginally significant effects, while the pattern no longer held for the histidine auxotroph (Δ*hisD*; $p > 0.05$; Table 2). Next, we removed the effect of AAD on the metabolic distances and repeated the regression analysis. In this case, recipient growth still correlated with the resulting values for *A. baylyi* (Δ*hisD*, $R^2 = 0.12$, $p < 0.0001$; Δ*trpB*, $R^2 = 0.12$, $p < 0.0001$), but not for *E. coli* (Δ*hisD*, $R^2 = 0.01$, $p > 0.05$; Δ*trpB*, $R^2 = 0.02$, $p > 0.05$).

After that, we asked whether the amount of amino acid produced by donors was sufficient to explain the growth observed in auxotrophic recipients. One possibility was that the positive association between the three distances measures (i.e., AAD,

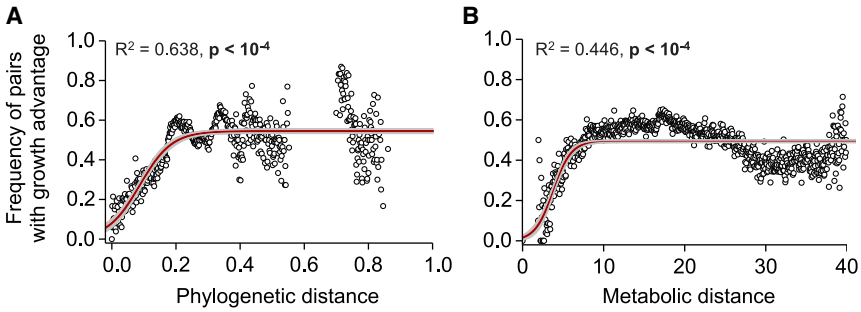

Figure 4. Metabolic simulations of gut bacterial cocultures predict a growth advantage that increases with increasing metabolic and phylogenetic distance

Shown are the results of an *in silico* flux-balance analysis of paired models analyzing 334,153 combinations of 818 bacterial species co-occurring in the human gut. A pair of species is considered as a pair with growth advantage if at least one of the two organisms is predicted to grow better in cocultures as compared to the predicted growth rate in monoculture. The frequency of pairs with growth advantage is estimated as a function of the (A) phylogenetic and (B) metabolic distance by defining 1,000 buckets of uniform distance widths spanning the range from 0 to the largest distance. Bucket values are only shown and included in logistic curve fitting if the bucket included at least ten species pairs. The red line shows the optimal fit of a logistic model to the data with the SE interval as gray ribbon (see also Table S1).

PD, and MD) with recipient growth could have, in fact, been only due to a positive correlation of these parameters with the amount of amino acids produced by donor genotypes. To control for this, we first calculated a linear regression for both AAD, PD, and MD with the TAAs or the amount of the FAA produced as the independent variable. The residuals (i.e., the variation not explained by TAA or FAA) were used as independent variables in these regressions. In almost all cases, recipients' growth remained significantly positively associated with the three distance measures (Table 2). Together, the set of analyses performed demonstrates that the three different measures analyzed (i.e., AAD, PD, and MD) can individually (in the case of *E. coli*) or in combination (both species) explain cross-feeding between prototrophic donors and auxotrophic recipients, thus corroborating the dissimilarity hypothesis.

In silico model confirms that the metabolic dissimilarity between species enhances cross-feeding

To verify whether the patterns observed in laboratory-based coculture experiments also applied to natural microbial communities, *in silico* modeling was used to simulate the co-growth of different bacterial species that co-occur in the human gastrointestinal tract. Specifically, all 334,153 pairwise combinations of 818 bacteria commonly found in this environment were considered. Co-growth phenotypes were predicted by, first, pairing the individual models of two strains to enable the potential exchange of metabolites between the two metabolic networks and, second, by maximizing the total biomass production (i.e., growth) as the sum of both strains' biomass formation rate. This approach of pairing models for co-growth simulations yields predictions on the potential ecological interactions between two organisms by comparing the growth predictions of the organisms in isolation and under co-growth conditions.[62] These *in silico* simulations indicated that the relationship between both phylogenetic and metabolic distance, and the frequency of pairs, for which at least one of the organisms gains a growth advantage from a metabolic interaction in coculture, follows a saturation curve (Figure 4; Table S1). This finding shows that bacteria residing within the human gut are more likely to engage in cross-feeding interactions with metabolically more dissimilar species. Taken together, the set of computational analyses performed is in line with the experimental data shown above: both datasets reveal that metabolic cross-feeding interactions are more likely to establish between two metabolically more dissimilar partners.

DISCUSSION

Metabolic cross-feeding interactions among different microbial species are ubiquitous and play critical roles in determining the structure and function of microbial communities.[16,63,64] However, the rules that govern their establishment remain poorly understood. Here, we identify the metabolic dissimilarity between donor and recipient genotype as a major determinant for the establishment of obligate, unidirectional cross-feeding interactions between two bacterial strains. In systematic coculture experiments between a prototrophic amino acid donor and an auxotrophic amino acid recipient, we show that growth of auxotrophic recipients in coculture was positively associated with (1) the compositional difference in the amino acid mixtures various donors produced (Figure 3A), (2) their phylogenetic distance (Figure 3B), as well as (3) the difference in their predicted metabolic networks (i.e., their metabolic distance; Figure 3C). Furthermore, *in silico* simulations of the co-growth of species from a gut microbial community corroborated that the propensity of cross-feeding interactions to establish increased when both interacting partners were metabolically more dissimilar (Figure 4).

In our study, we manipulated the relatedness between donor and recipient genotypes by performing experiments with strains that differed in this parameter. A high phylogenetic relatedness between two genotypes (donor and recipient) in coculture means that they are more likely to be characterized by overlapping growth requirements.[33,47] As a consequence, a high relatedness between donor and recipient aggravates the extent of exploitative competition for limiting resources between partners.[54] Moreover, the physiological costs to produce a given metabolite is more similar between two genetically related bacterial cells than between two more distantly related individuals.[47,65,66] Assuming that donors should predominantly release metabolites that have a lower nutritional value for themselves, auxotrophic recipients are more likely to obtain the required metabolite when interacting with heterospecific donors.[57,58,67] These statistical relationships can explain why, in our coculture experiments, both the phylogenetic and metabolic distance were positively associated with the growth of cocultured auxotrophs. Thus, our results support the dissimilarity hypothesis to

explain the establishment of unidirectional cross-feeding interactions. Our findings align with previous studies that analyzed the effect of the phylogenetic relatedness and metabolic dissimilarity on antagonistic interactions between two different genotypes. These studies found that bacteria mainly inhibit the growth of metabolically more similar and related species.[45,68] Even though the focal biological process differs drastically between our (metabolic cross-feeding) and these other studies (antagonistic interactions), the main finding is conceptually equivalent: genotypes are more likely to compete against closer relatives yet support the growth of more dissimilar strains—either by enhancing their growth (Figure 3) or inhibiting them less.[45,68,69] In addition, our results can help explain the repeatedly observed positive association between the productivity of a microbial community and the phylogenetic distance among its members:[69,70] strains within diverse communities are more likely to engage in synergistic cross-feeding of metabolites than those of less diverse communities (this study), which in turn can increase the total productivity of these communities.[48]

Our experiments took advantage of synthetically assembled pairwise interactions between different bacterial genotypes to assess how the similarity between interacting partners affects the cross-feeding of metabolites. Even though this approach is limited by the number of pairwise comparisons that can be analyzed in one experiment, the obtained results provide a very clear answer to the focal question. First, the selected donor strains covered a broad range of taxonomic diversity in bacteria (Figure 1B). Thus, the spectrum of ecological interactions analyzed here likely reflects the range of interactions a given bacterial genotype would typically experience in a natural microbial community. Second, by choosing strains such that the possibility of previous coevolutionary history is minimized, any result observed can be attributed to the focal, experimentally controlled parameter (e.g., phylogenetic or metabolic distance). In this way, confounding effects like an evolved preference for a particular genotype can most likely be ruled out. Finally, we analyzed bacterial consortia in a well-mixed, spatially unstructured environment, in which the exchanged metabolites are transferred between cells via diffusion through the extracellular environment. Such a setup minimizes factors that would be amplified in a spatially structured environment, such as a local competition for nutrients or the release of metabolic waste products that inhibit the growth of other cells in the local vicinity. Thus, the experimental approach chosen circumvents the challenges of manipulating and detecting metabolite exchange in natural environments and instead capitalizes on analyzing experimentally arranged and carefully controlled coculture experiments.

However, the identified metabolic dissimilarity between two strains is likely not the only factor driving the establishment of metabolic cross-feeding interactions. For example, growth in spatially structured environments can significantly affect the mixing among different genotypes and thus also the probability of cross-feeding interactions to emerge.[71,72] Other mechanisms include positive chemotaxis towards suitable partner genotypes,[73] direct cell-cell attachment,[36,74] or antagonistic behaviors, such as the preferential killing of certain strains.[75] Thus, in natural microbial communities, the successful establishment of a metabolic cross-feeding interaction likely depends on the dynamic interplay between the metabolic dissimilarity between strains, the frequency of suitable interaction partners, and the other above-mentioned mechanisms.

The guiding principle discovered in this study is most likely relevant for ecological interactions outside the realm of microbial communities. Mutualistic interactions, in which two partners reciprocally exchange essential metabolites or services, usually involve two or more completely unrelated species.[65,76–78] In contrast, cooperative interactions among closely related individuals usually rely on the uni- or bidirectional exchange of the same commodity or service.[65] Thus, the finding that two more dissimilar individuals have an increased potential to engage in a synergistic interaction over two more similar individuals may be a universal rule that guides the establishment of mutualistic interactions in general.[47]

Our results highlight the utility of using synthetic, laboratory-based model systems to understand the fundamental principles of microbial ecology. In this study, we demonstrated that simple assembly rules are likely to determine the establishment of interactions in natural microbial communities. These insights enrich our understanding of the complex relationships among bacteria in their natural environment and will help to rationally design and modify them for biotechnological or medical applications.

STAR★METHODS

Detailed methods are provided in the online version of this paper and include the following:

- KEY RESOURCES TABLE
- RESOURCE AVAILABILITY
  - Lead contact
  - Materials availability
  - Data and code availability
- EXPERIMENTAL MODEL AND SUBJECT DETAILS
  - Bacterial strains and their construction
  - Soil sampling, bacterial isolation, 16S rRNA gene amplification, and taxonomic affiliation
- METHOD DETAILS
  - Culture conditions and general procedures
  - Coculture experiment
  - Relative fitness measurement
  - Amino acid supernatant experiment
  - Amino acid quantification by LC-MS/MS
  - Amino acid profile-based distance calculation using supernatant data
  - Phylogenetic tree construction and distance calculation
  - Reconstruction of metabolic networks
  - Calculating the genome-based metabolic distance of organisms
  - *In silico* simulation of bacterial co-growth
- QUANTIFICATION AND STATISTICAL ANALYSIS

SUPPLEMENTAL INFORMATION

Supplemental information can be found online at https://doi.org/10.1016/j.cub.2021.10.019.

ACKNOWLEDGMENTS

We thank the entire Kost lab (past and present) for useful discussion, as well as Marita Hermann and Antje Möhlmeyer for technical assistance. We are grateful to Stefan Walter and Saskia Schuback (CellNanOS, MS facility) for help with quantifying the exo-metabolome, Heiko Vogel and Domenica Schnabelrauch (Department of Entomology, MPI-CE) for help with 16S rRNA sequencing, Ákos T. Kovács (Technical University of Denmark, Denmark) for sharing two *Bacillus subtilis* strains, and Michael Hensel (Department of Microbiology, University of Osnabrück, Germany) for providing *Serratia ficaria*. Comments and suggestions of three anonymous reviewers on earlier versions of the manuscript are gratefully acknowledged. This work was funded by the German Research Foundation (SPP1617 and KO 3909/2-1: C. Kost and S.G.; SFB 944 and P19: C. Kost; KO 3909/4-1: C. Kost), DAAD GERLS program (G.Y. and C. Kost), and the University of Osnabrück (S.G., L.O., and G.Y.; *EvoCell*: C. Kost). C. Kaleta and S.W. acknowledge support by the German Research Foundation within the scope of the Excellence Cluster "Precision medicine in chronic inflammation" (EXC2167, sub-project RTF-VIII) and the Collaborative Research Center "Metaorganisms" (SFB1182, sub-project A1).

AUTHOR CONTRIBUTIONS

Conceptualization, S.G. and C. Kost; methodology, S.G., S.S., S.W., C. Kaleta, and C. Kost; formal analysis, S.G., L.O., and S.W.; investigation, S.G., S.W., and G.Y.; writing – original draft, S.G. and C. Kost; writing – review & editing, S.G., C. Kost, L.O., S.W., S.S., and G.Y.; visualization, S.G., L.O., S.W., and S.S.; resources, project administration, and funding acquisition, C. Kost.

DECLARATION OF INTERESTS

The authors declare no competing interests.

Received: March 6, 2021
Revised: September 1, 2021
Accepted: October 8, 2021
Published: November 2, 2021

REFERENCES

1. Fierer, N., and Jackson, R.B. (2006). The diversity and biogeography of soil bacterial communities. Proc. Natl. Acad. Sci. USA *103*, 626–631.
2. Lozupone, C.A., and Knight, R. (2007). Global patterns in bacterial diversity. Proc. Natl. Acad. Sci. USA *104*, 11436–11440.
3. Falkowski, P.G., Fenchel, T., and Delong, E.F. (2008). The microbial engines that drive Earth's biogeochemical cycles. Science *320*, 1034–1039.
4. Fierer, N. (2017). Embracing the unknown: disentangling the complexities of the soil microbiome. Nat. Rev. Microbiol. *15*, 579–590.
5. Mendes, R., Kruijt, M., de Bruijn, I., Dekkers, E., van der Voort, M., Schneider, J.H.M., Piceno, Y.M., DeSantis, T.Z., Andersen, G.L., Bakker, P.A.H.M., and Raaijmakers, J.M. (2011). Deciphering the rhizosphere microbiome for disease-suppressive bacteria. Science *332*, 1097–1100.
6. Saleem, M., Hu, J., and Jousset, A. (2019). More than the sum of its parts: microbiome biodiversity as a driver of plant growth and soil health. Annu. Rev. Ecol. Evol. Syst. *50*, 145–168.
7. Russell, C.W., Poliakov, A., Haribal, M., Jander, G., van Wijk, K.J., and Douglas, A.E. (2014). Matching the supply of bacterial nutrients to the nutritional demand of the animal host. Proc. Biol. Sci. *281*, 20141163.
8. Kwong, W.K., Medina, L.A., Koch, H., Sing, K.-W., Soh, E.J.Y., Ascher, J.S., Jaffé, R., and Moran, N.A. (2017). Dynamic microbiome evolution in social bees. Sci. Adv. *3*, e1600513.
9. Kau, A.L., Ahern, P.P., Griffin, N.W., Goodman, A.L., and Gordon, J.I. (2011). Human nutrition, the gut microbiome and the immune system. Nature *474*, 327–336.
10. Lynch, S.V., and Pedersen, O. (2016). The human intestinal microbiome in health and disease. N. Engl. J. Med. *375*, 2369–2379.
11. Leventhal, G.E., Boix, C., Kuechler, U., Enke, T.N., Sliwerska, E., Holliger, C., and Cordero, O.X. (2018). Strain-level diversity drives alternative community types in millimetre-scale granular biofilms. Nat. Microbiol. *3*, 1295–1303.
12. Rivett, D.W., and Bell, T. (2018). Abundance determines the functional role of bacterial phylotypes in complex communities. Nat. Microbiol. *3*, 767–772.
13. Giri, S., Shitut, S., and Kost, C. (2020). Harnessing ecological and evolutionary principles to guide the design of microbial production consortia. Curr. Opin. Biotechnol. *62*, 228–238.
14. Kong, W., Meldgin, D.R., Collins, J.J., and Lu, T. (2018). Designing microbial consortia with defined social interactions. Nat. Chem. Biol. *14*, 821–829.
15. Rezzoagli, C., Granato, E.T., and Kümmerli, R. (2020). Harnessing bacterial interactions to manage infections: a review on the opportunistic pathogen *Pseudomonas aeruginosa* as a case example. J. Med. Microbiol. *69*, 147–161.
16. D'Souza, G., Shitut, S., Preussger, D., Yousif, G., Waschina, S., and Kost, C. (2018). Ecology and evolution of metabolic cross-feeding interactions in bacteria. Nat. Prod. Rep. *35*, 455–488.
17. Zengler, K., and Zaramela, L.S. (2018). The social network of microorganisms - how auxotrophies shape complex communities. Nat. Rev. Microbiol. *16*, 383–390.
18. Cordero, O.X., and Datta, M.S. (2016). Microbial interactions and community assembly at microscales. Curr. Opin. Microbiol. *31*, 227–234.
19. Enke, T.N., Datta, M.S., Schwartzman, J., Cermak, N., Schmitz, D., Barrere, J., Pascual-García, A., and Cordero, O.X. (2019). Modular assembly of polysaccharide-degrading marine microbial communities. Curr. Biol. *29*, 1528–1535.e6.
20. Sieuwerts, S., Molenaar, D., van Hijum, S.A.F.T., Beerthuyzen, M., Stevens, M.J.A., Janssen, P.W.M., Ingham, C.J., de Bok, F.A.M., de Vos, W.M., and van Hylckama Vlieg, J.E.T. (2010). Mixed-culture transcriptome analysis reveals the molecular basis of mixed-culture growth in *Streptococcus thermophilus* and *Lactobacillus bulgaricus*. Appl. Environ. Microbiol. *76*, 7775–7784.
21. Ponomarova, O., Gabrielli, N., Sévin, D.C., Mülleder, M., Zirngibl, K., Bulyha, K., Andrejev, S., Kafkia, E., Typas, A., Sauer, U., et al. (2017). Yeast creates a niche for symbiotic lactic acid bacteria through nitrogen overflow. Cell Syst. *5*, 345–357.e6.
22. Croft, M.T., Lawrence, A.D., Raux-Deery, E., Warren, M.J., and Smith, A.G. (2005). Algae acquire vitamin B_{12} through a symbiotic relationship with bacteria. Nature *438*, 90–93.
23. Sokolovskaya, O.M., Shelton, A.N., and Taga, M.E. (2020). Sharing vitamins: cobamides unveil microbial interactions. Science *369*, eaba0165.
24. Loera-Muro, A., Jacques, M., Avelar-González, F.J., Labrie, J., Tremblay, Y.D.N., Oropeza-Navarro, R., and Guerrero-Barrera, A.L. (2016). Auxotrophic *Actinobacillus pleurpneumoniae* grows in multispecies biofilms without the need for nicotinamide-adenine dinucleotide (NAD) supplementation. BMC Microbiol. *16*, 128.
25. Rakoff-Nahoum, S., Coyne, M.J., and Comstock, L.E. (2014). An ecological network of polysaccharide utilization among human intestinal symbionts. Curr. Biol. *24*, 40–49.
26. Paczia, N., Nilgen, A., Lehmann, T., Gätgens, J., Wiechert, W., and Noack, S. (2012). Extensive exometabolome analysis reveals extended overflow metabolism in various microorganisms. Microb. Cell Fact. *11*, 122.
27. Douglas, A.E. (2020). The microbial exometabolome: ecological resource and architect of microbial communities. Philos. Trans. R. Soc. Lond. B Biol. Sci. *375*, 20190250.
28. Campbell, K., Herrera-Dominguez, L., Correia-Melo, C., Zelezniak, A., and Ralser, M. (2018). Biochemical principles enabling metabolic cooperativity and phenotypic heterogeneity at the single cell level. Curr. Opin. Syst. Biol. *8*, 97–108.

29. Schink, B. (2002). Synergistic interactions in the microbial world. Antonie van Leeuwenhoek *81*, 257–261.

30. Morris, J.J. (2015). Black Queen evolution: the role of leakiness in structuring microbial communities. Trends Genet. *31*, 475–482.

31. Cordero, O.X., Ventouras, L.-A., DeLong, E.F., and Polz, M.F. (2012). Public good dynamics drive evolution of iron acquisition strategies in natural bacterioplankton populations. Proc. Natl. Acad. Sci. USA *109*, 20059–20064.

32. Schuster, M., Sexton, D.J., Diggle, S.P., and Greenberg, E.P. (2013). Acyl-homoserine lactone quorum sensing: from evolution to application. Annu. Rev. Microbiol. *67*, 43–63.

33. Zelezniak, A., Andrejev, S., Ponomarova, O., Mende, D.R., Bork, P., and Patil, K.R. (2015). Metabolic dependencies drive species co-occurrence in diverse microbial communities. Proc. Natl. Acad. Sci. USA *112*, 6449–6454.

34. Giri, S., Waschina, S., Kaleta, C., and Kost, C. (2019). Defining division of labor in microbial communities. J. Mol. Biol. *431*, 4712–4731.

35. Giovannoni, S.J., Cameron Thrash, J., and Temperton, B. (2014). Implications of streamlining theory for microbial ecology. ISME J. *8*, 1553–1565.

36. Pande, S., Shitut, S., Freund, L., Westermann, M., Bertels, F., Colesie, C., Bischofs, I.B., and Kost, C. (2015). Metabolic cross-feeding via intercellular nanotubes among bacteria. Nat. Commun. *6*, 6238.

37. Sanchez, A., and Gore, J. (2013). feedback between population and evolutionary dynamics determines the fate of social microbial populations. PLoS Biol. *11*, e1001547.

38. MacLean, R.C., and Gudelj, I. (2006). Resource competition and social conflict in experimental populations of yeast. Nature *441*, 498–501.

39. D'Souza, G., and Kost, C. (2016). Experimental evolution of metabolic dependency in bacteria. PLoS Genet. *12*, e1006364.

40. Baran, R., Brodie, E.L., Mayberry-Lewis, J., Hummel, E., Da Rocha, U.N., Chakraborty, R., Bowen, B.P., Karaoz, U., Cadillo-Quiroz, H., Garcia-Pichel, F., and Northen, T.R. (2015). Exometabolite niche partitioning among sympatric soil bacteria. Nat. Commun. *6*, 8289.

41. Butaitė, E., Baumgartner, M., Wyder, S., and Kümmerli, R. (2017). Siderophore cheating and cheating resistance shape competition for iron in soil and freshwater *Pseudomonas* communities. Nat. Commun. *8*, 414.

42. Garcia, S.L., Buck, M., McMahon, K.D., Grossart, H.-P., Eiler, A., and Warnecke, F. (2015). Auxotrophy and intrapopulation complementary in the 'interactome' of a cultivated freshwater model community. Mol. Ecol. *24*, 4449–4459.

43. Macdonald, S.J., Lin, G.G., Russell, C.W., Thomas, G.H., and Douglas, A.E. (2012). The central role of the host cell in symbiotic nitrogen metabolism. Proc. Biol. Sci. *279*, 2965–2973.

44. Narwani, A., Alexandrou, M.A., Oakley, T.H., Carroll, I.T., and Cardinale, B.J. (2013). Experimental evidence that evolutionary relatedness does not affect the ecological mechanisms of coexistence in freshwater green algae. Ecol. Lett. *16*, 1373–1381.

45. Russel, J., Røder, H.L., Madsen, J.S., Burmølle, M., and Sørensen, S.J. (2017). Antagonism correlates with metabolic similarity in diverse bacteria. Proc. Natl. Acad. Sci. USA *114*, 10684–10688.

46. Xenophontos, C., Taubert, M., Harpole, W.S., and Küsel, K. (2021). Phylogenetic and metabolic diversity have contrasting effects on the ecological functioning of bacterial communities. FEMS Microbiol. Ecol. *97*, fiab017.

47. Machado, D., Maistrenko, O.M., Andrejev, S., Kim, Y., Bork, P., Patil, K.R., and Patil, K.R. (2021). Polarization of microbial communities between competitive and cooperative metabolism. Nat. Ecol. Evol. *5*, 195–203.

48. Shitut, S., Ahsendorf, T., Pande, S., Egbert, M., and Kost, C. (2019). Nanotube-mediated cross-feeding couples the metabolism of interacting bacterial cells. Environ. Microbiol. *21*, 1306–1320.

49. Troselj, V., Cao, P., and Wall, D. (2018). Cell-cell recognition and social networking in bacteria. Environ. Microbiol. *20*, 923–933.

50. Stefanic, P., Decorosi, F., Viti, C., Petito, J., Cohan, F.M., and Mandic-Mulec, I. (2012). The quorum sensing diversity within and between ecotypes of *Bacillus subtilis*. Environ. Microbiol. *14*, 1378–1389.

51. Ranava, D., Backes, C., Karthikeyan, G., Ouari, O., Soric, A., Guiral, M., Cárdenas, M.L., and Giudici-Orticoni, M.T. (2021). Metabolic exchange and energetic coupling between nutritionally stressed bacterial species: role of quorum-sensing molecules. MBio *12*, e02758-20.

52. Macarthur, R., and Levins, R. (1967). The limiting similarity, convergence, and divergence of coexisting species. Am. Nat. *101*, 377–385.

53. Mayfield, M.M., and Levine, J.M. (2010). Opposing effects of competitive exclusion on the phylogenetic structure of communities. Ecol. Lett. *13*, 1085–1093.

54. Mitri, S., and Foster, K.R. (2013). The genotypic view of social interactions in microbial communities. Annu. Rev. Genet. *47*, 247–273.

55. Bernhardsson, S., Gerlee, P., and Lizana, L. (2011). Structural correlations in bacterial metabolic networks. BMC Evol. Biol. *11*, 20.

56. Hester, E.R., Jetten, M.S.M., Welte, C.U., and Lücker, S. (2019). Metabolic overlap in environmentally diverse microbial communities. Front. Genet. *10*, 989.

57. Waschina, S., D'Souza, G., Kost, C., and Kaleta, C. (2016). Metabolic network architecture and carbon source determine metabolite production costs. FEBS J. *283*, 2149–2163.

58. Akashi, H., and Gojobori, T. (2002). Metabolic efficiency and amino acid composition in the proteomes of *Escherichia coli* and *Bacillus subtilis*. Proc. Natl. Acad. Sci. USA *99*, 3695–3700.

59. Zakataeva, N.P., Aleshin, V.V., Tokmakova, I.L., Troshin, P.V., and Livshits, V.A. (1999). The novel transmembrane *Escherichia coli* proteins involved in the amino acid efflux. FEBS Lett. *452*, 228–232.

60. Doroshenko, V., Airich, L., Vitushkina, M., Kolokolova, A., Livshits, V., and Mashko, S. (2007). YddG from *Escherichia coli* promotes export of aromatic amino acids. FEMS Microbiol. Lett. *275*, 312–318.

61. Airich, L.G., Tsyrenzhapova, I.S., Vorontsova, O.V., Feofanov, A.V., Doroshenko, V.G., and Mashko, S.V. (2010). Membrane topology analysis of the *Escherichia coli* aromatic amino acid efflux protein YddG. J. Mol. Microbiol. Biotechnol. *19*, 189–197.

62. Heinken, A., Sahoo, S., Fleming, R.M.T., and Thiele, I. (2013). Systems-level characterization of a host-microbe metabolic symbiosis in the mammalian gut. Gut Microbes *4*, 28–40.

63. Morris, B.E.L., Henneberger, R., Huber, H., and Moissl-Eichinger, C. (2013). Microbial syntrophy: interaction for the common good. FEMS Microbiol. Rev. *37*, 384–406.

64. Ponomarova, O., and Patil, K.R. (2015). Metabolic interactions in microbial communities: untangling the Gordian knot. Curr. Opin. Microbiol. *27*, 37–44.

65. Barker, J.L., Bronstein, J.L., Friesen, M.L., Jones, E.I., Reeve, H.K., Zink, A.G., and Frederickson, M.E. (2017). Synthesizing perspectives on the evolution of cooperation within and between species. Evolution *71*, 814–825.

66. Oña, L., Giri, S., Avermann, N., Kreienbaum, M., Thormann, K.M., and Kost, C. (2021). Obligate cross-feeding expands the metabolic niche of bacteria. Nat. Ecol. Evol. *5*, 1224–1232.

67. Swire, J. (2007). Selection on synthesis cost affects interprotein amino acid usage in all three domains of life. J. Mol. Evol. *64*, 558–571.

68. Westhoff, S., Kloosterman, A.M., van Hoesel, S.F.A., van Wezel, G.P., and Rozen, D.E. (2021). Competition sensing changes antibiotic production in *Streptomyces*. MBio *12*, e02729-20.

69. Venail, P.A., and Vives, M.J. (2013). Phylogenetic distance and species richness interactively affect the productivity of bacterial communities. Ecology *94*, 2529–2536.

70. Galand, P.E., Salter, I., and Kalenitchenko, D. (2015). Ecosystem productivity is associated with bacterial phylogenetic distance in surface marine waters. Mol. Ecol. *24*, 5785–5795.

71. Pande, S., Kaftan, F., Lang, S., Svatoš, A., Germerodt, S., and Kost, C. (2016). Privatization of cooperative benefits stabilizes mutualistic cross-feeding interactions in spatially structured environments. ISME J. *10*, 1413–1423.

72. Germerodt, S., Bohl, K., Lück, A., Pande, S., Schröter, A., Kaleta, C., Schuster, S., and Kost, C. (2016). Pervasive selection for cooperative cross-feeding in bacterial communities. PLoS Comput. Biol. *12*, e1004986.

73. Yang, Y., M Pollard, A., Höfler, C., Poschet, G., Wirtz, M., Hell, R., and Sourjik, V. (2015). Relation between chemotaxis and consumption of amino acids in bacteria. Mol. Microbiol. *96*, 1272–1282.

74. Konovalova, A., and Søgaard-Andersen, L. (2011). Close encounters: contact-dependent interactions in bacteria. Mol. Microbiol. *81*, 297–301.

75. Granato, E.T., Meiller-Legrand, T.A., and Foster, K.R. (2019). The evolution and ecology of bacterial warfare. Curr. Biol. *29*, R521–R537.

76. Bronstein, J.L. (1994). Our current understanding of mutualism. Q. Rev. Biol. *69*, 31–51.

77. Kiers, E.T., Rousseau, R.A., West, S.A., and Denison, R.F. (2003). Host sanctions and the legume-rhizobium mutualism. Nature *425*, 78–81.

78. McFall-Ngai, M. (2008). Hawaiian bobtail squid. Curr. Biol. *18*, R1043–R1044.

79. D'Souza, G., Waschina, S., Pande, S., Bohl, K., Kaleta, C., and Kost, C. (2014). Less is more: selective advantages can explain the prevalent loss of biosynthetic genes in bacteria. Evolution *68*, 2559–2570.

80. Vaneechoutte, M., Young, D.M., Ornston, L.N., De Baere, T., Nemec, A., Van Der Reijden, T., Carr, E., Tjernberg, I., and Dijkshoorn, L. (2006). Naturally transformable Acinetobacter sp. strain ADP1 belongs to the newly described species Acinetobacter baylyi. Appl. Environ. Microbiol. *72*, 932–936.

81. Konkol, M.A., Blair, K.M., and Kearns, D.B. (2013). Plasmid-encoded ComI inhibits competence in the ancestral 3610 strain of *Bacillus subtilis*. J. Bacteriol. *195*, 4085–4093.

82. Nicolas, P., Mäder, U., Dervyn, E., Rochat, T., Leduc, A., Pigeonneau, N., Bidnenko, E., Marchadier, E., Hoebeke, M., Aymerich, S., et al. (2012). Condition-dependent transcriptome reveals high-level regulatory architecture in *Bacillus subtilis*. Science *335*, 1103–1106.

83. Baba, T., Ara, T., Hasegawa, M., Takai, Y., Okumura, Y., Baba, M., Datsenko, K.A., Tomita, M., Wanner, B.L., and Mori, H. (2006). Construction of Escherichia coli K-12 in-frame, single-gene knockout mutants: the Keio collection. Mol. Syst. Biol. *2*, 2006.0008.

84. Thompson, I.P., Lilley, A.K., Ellis, R.J., Bramwell, P.A., and Bailey, M.J. (1995). Survival, colonization and dispersal of genetically modified *Pseudomonas fluorescens* SBW25 in the phytosphere of field grown sugar beet. Nat. Biotechnol. *13*, 1493–1497.

85. Kumar, S., Stecher, G., Li, M., Knyaz, C., and Tamura, K. (2018). MEGA X: Molecular evolutionary genetics analysis across computing platforms. Mol. Biol. Evol. *35*, 1547–1549.

86. Letunic, I., and Bork, P. (2007). Interactive Tree Of Life (iTOL): an online tool for phylogenetic tree display and annotation. Bioinformatics *23*, 127–128.

87. R Development Core Team (2013). R: A language and environment for statistical computing (R Foundation for Statistical Computing).

88. Ogata, H., Goto, S., Sato, K., Fujibuchi, W., Bono, H., and Kanehisa, M. (1999). KEGG: Kyoto encyclopedia of genes and genomes. Nucleic Acids Res. *27*, 29–34.

89. Keseler, I.M., Collado-Vides, J., Santos-Zavaleta, A., Peralta-Gil, M., Gama-Castro, S., Muñiz-Rascado, L., Bonavides-Martinez, C., Paley, S., Krummenacker, M., Altman, T., et al. (2011). EcoCyc: a comprehensive database of *Escherichia coli* biology. Nucleic Acids Res. *39*, D583–D590.

90. Thomason, L.C., Costantino, N., and Court, D.L. (2007). E. coli genome manipulation by P1 transduction. Curr. Protoc. Mol. Biol. *79*, 1.17.1–1.17.8.

91. Joyce, A.R., Reed, J.L., White, A., Edwards, R., Osterman, A., Baba, T., Mori, H., Lesely, S.A., Palsson, B.Ø., and Agarwalla, S. (2006). Experimental and computational assessment of conditionally essential genes in *Escherichia coli*. J. Bacteriol. *188*, 8259–8271.

92. Weisburg, W.G., Barns, S.M., Pelletier, D.A., and Lane, D.J. (1991). 16S ribosomal DNA amplification for phylogenetic study. J. Bacteriol. *173*, 697–703.

93. Altschul, S.F., Gish, W., Miller, W., Myers, E.W., and Lipman, D.J. (1990). Basic local alignment search tool. J. Mol. Biol. *215*, 403–410.

94. Vanstockem, M., Michiels, K., Vanderleyden, J., and Van Gool, A.P. (1987). Transposon mutagenesis of *Azospirillum brasilense* and *Azospirillum lipoferum*: physical analysis of Tn5 and Tn5-Mob insertion mutants. Appl. Environ. Microbiol. *53*, 410–415.

95. Tapuhi, Y., Schmidt, D.E., Lindner, W., and Karger, B.L. (1981). Dansylation of amino acids for high-performance liquid chromatography analysis. Anal. Biochem. *115*, 123–129.

96. Takeuchi, T. (2005). 1.2.5. - HPLC of amino acids as dansyl and dabsyl derivatives. J. Chromatogr. Lib. *70*, 229–241.

97. Zimmermann, J., Kaleta, C., and Waschina, S. (2021). gapseq: informed prediction of bacterial metabolic pathways and reconstruction of accurate metabolic models. Genome Biol. *22*, 81.

98. Karp, P.D., Riley, M., Paley, S.M., and Pellegrini-Toole, A. (2002). The MetaCyc Database. Nucleic Acids Res. *30*, 59–61.

99. Boutet, E., Lieberherr, D., Tognolli, M., Schneider, M., and Bairoch, A. (2007). UniProtKB/Swiss-Prot. In Plant Bioinformatics: Methods and Protocols, D. Edwards, ed. (Humana), pp. 89–112.

100. Ye, J., McGinnis, S., and Madden, T.L. (2006). BLAST: improvements for better sequence analysis. Nucleic Acids Res. *34*, W6–W9.

101. Devoid, S., Overbeek, R., DeJongh, M., Vonstein, V., Best, A.A., and Henry, C. (2013). Automated genome annotation and metabolic model reconstruction in the SEED and model SEED. In Systems Metabolic Engineering: Methods and Protocols, H.S. Alper, ed. (Humana), pp. 17–45.

102. Holzhütter, H.-G. (2004). The principle of flux minimization and its application to estimate stationary fluxes in metabolic networks. Eur. J. Biochem. *271*, 2905–2922.

103. Magnúsdóttir, S., Heinken, A., Kutt, L., Ravcheev, D.A., Bauer, E., Noronha, A., Greenhalgh, K., Jäger, C., Baginska, J., Wilmes, P., et al. (2017). Generation of genome-scale metabolic reconstructions for 773 members of the human gut microbiota. Nat. Biotechnol. *35*, 81–89.

104. Aden, K., Rehman, A., Waschina, S., Pan, W.-H., Walker, A., Lucio, M., Nunez, A.M., Bharti, R., Zimmerman, J., Bethge, J., et al. (2019). Metabolic functions of gut microbes associate with efficacy of tumor necrosis factor antagonists in patients with inflammatory bowel diseases. Gastroenterology *157*, 1279–1292.e11.

105. Mirhakkak, M.H., Schäuble, S., Klassert, T.E., Brunke, S., Brandt, P., Loos, D., Uribe, R.V., Senne de Oliveira Lino, F., Ni, Y., Vylkova, S., et al. (2020). Metabolic modeling predicts specific gut bacteria as key determinants for *Candida albicans* colonization levels. ISME J. *15*, 1257–1270.

106. Benjamini, Y., and Hochberg, Y. (1995). Controlling the false discovery rate: a practical and powerful approach to multiple testing. J. R. Stat. Soc. B *57*, 289–300.

107. Benjamini, Y., Krieger, A.M., and Yekutieli, D. (2006). Adaptive linear step-up procedures that control the false discovery rate. Biometrika *93*, 491–507.

108. Menard, S.W. (1995). Applied Logistic Regression Analysis (Sage).

STAR★METHODS

KEY RESOURCES TABLE

REAGENT or RESOURCE	SOURCE	IDENTIFIER
Chemicals, peptides, and recombinant proteins		
Lysogeny broth (LB), Lennox	Carl Roth GmbH	Catalog # X964.1
Agar-Agar Kobe	Carl Roth GmbH	Catalog # 5210.2
Dipotassium hydrogen phosphate	Carl Roth GmbH	Catalog # 26931.263
Sodium dihydrogen phosphate	Carl Roth GmbH	Catalog # T879.2
Magnesium sulfate heptahydrate	Carl Roth GmbH	Catalog # P027.2
Potassium chloride	VWR	Catalog # 26764.260
Calcium chloride dihydrate	Carl Roth GmbH	Catalog # 5239.2
Ammonium chloride	VWR	Catalog # 21236.267
Iron (II) sulfate heptahydrate	Merck	Catalog # 3965
Manganese chloride	AppliChem	Catalog # A2087.0100
Cobalt chloride hexahydrate	AppliChem	Catalog # A2087.0100
Boric acid	Carl Roth GmbH	Catalog # 6943.3
Nickel chloride	AppliChem	Catalog # A3917.0100
Zinc sulfate heptahydrate	Carl Roth GmbH	Catalog # K301.1
Copper chloride dihydrate	AppliChem	Catalog # 131264.1210
Glucose	Carl Roth GmbH	Catalog # 6887.1
Kanamycin	Carl Roth GmbH	Catalog # T832.2
Sodium carbonate	Merck	Catalog # 1063920.500
Acetonitrile	Sigma-Aldrich	Catalog # 271004
Formic acid	Acros-Organics	Catalog # 270480250
L-Alanine	AppliChem reagents	Catalog # A3690,0100
L-Arginine monohydrochloride	AppliChem reagents	Catalog # A3709,0100
L-Asparagine monohydrochloride	AppliChem reagents	Catalog # A3721,0100
L-Aspartic acid	AppliChem reagents	Catalog # A3715,0250
L-Cysteine monohydrochloride	AppliChem reagents	Catalog # A3694,0050
L-Glutamine monohydrochloride	AppliChem reagents	Catalog # A3734,0100
L-Glutamic acid monohydrochloride	AppliChem reagents	Catalog # A3712,0250
Glycine	AppliChem reagents	Catalog # A1067,1000
L-Histidine monohydrochloride	AppliChem reagents	Catalog # A3733,0100
L-Isoleucine	AppliChem reagents	Catalog # A1440,1000
L-Leucine	AppliChem reagents	Catalog # A3460,0100
L-Lysine monohydrochloride	AppliChem reagents	Catalog # A3466,0100
L-Methionine	AppliChem reagents	Catalog # A1340,0100
L-Phenylalanine	AppliChem reagents	Catalog # A3442,0100
L-Proline	AppliChem reagents	Catalog # A3453,0100
L-Serine	AppliChem reagents	Catalog # A3973,0100
L-Threonine	AppliChem reagents	Catalog # A3969,0100
L-Tryptophan	AppliChem reagents	Catalog # A3445,0100
L-Tyrosine disodium salt hydrate	Sigma	Catalog # T1145-25G
L-Valine	AppliChem reagents	Catalog # A1637,1000
48-well deep well plates	Axygen	Catalog # P-5ML-48-C-S
96-well deep well plates	Eppendorf	Catalog # 0030506308D
384-well plates	Greiner bio-one	Catalog # 781185
Plate sealer	Greiner bio-one	Catalog # 676070

(*Continued on next page*)

Continued

REAGENT or RESOURCE	SOURCE	IDENTIFIER
Petri dish	Greiner bio-one	Catalog # 633180
96 well Filter plates (0.2 μm PTFE membrane)	Pall AcroPrep	Catalog # 8047
Deposited data		
Peribacillus simplex	This study	GenBank: MW073531
Variovorax boronicumulans	This study	GenBank: MW073532
Cupriavidus metallidurans	This study	GenBank: MW073533
Bacillus licheniformis	This study	GenBank: MW073534
Nocardia coeliaca	This study	GenBank: MW080346-MW080347
Experimental models: Organisms/strains		
Donors		
Acinetobacter baylyi ADP1 (AB)	Lab stock	D'Souza et al.[79] and Vaneechoutte et al.[80]
Arthrobacter nicotianae (AN)	German Collection of Microorganisms and Cell Cultures, DSMZ	DSM 20123
Agrobacterium tumefaciens (AT)	Lab stock	Soil
Azospirillum brasilense (AZB)	German Collection of Microorganisms and Cell Cultures, DSMZ	DSM1690
Bacillus licheniformis (BL)	This study	Soil isolate from sample site coordinates 50.906557, 11.505631
Bacillus megaterium (BM)	German Collection of Microorganisms and Cell Cultures, DSMZ	DSM 32
Peribacillus simplex (BS)	This study	Soil isolate from sample site coordinates 50.906557, 11.505631
Bacillus subtilis 3610 *comI*^{Q12L} (BSN)	Konkol et al.[81]	Provided by Ákos T. Kovács, DTU
Bacillus subtilis 168 *trpc*$^{+}$ (BSS)	Nicolas et al.[82]	Provided by Ákos T. Kovács, DTU
Cupriavidus metallidurans (CM)	This study	Soil isolate from sample site coordinates 50.906557, 11.505631
Escherichia coli BW25113 (ECB)	Baba et al.[83]	*E. coli* Genetic resources at Yale CGSC, The Coli Genetic Stock Center
Escherichia coli MG1655 (ECM)	German Collection of Microorganisms and Cell Cultures, DSMZ	DSM 18039
Flavobacterium johnsoniae (FJ)	German Collection of Microorganisms and Cell Cultures, DSMZ	DSM 2064
Nocardia coeliaca (NC)	This study	Soil isolate from sample site coordinates 50.906557, 11.505631
Pseudomonas fluorescens (PF)	German Collection of Microorganisms and Cell Cultures, DSMZ	DSM 289
Pseudomonas fluorescense Pf-5 (PFP)	Lab stock	Soil
Pseudomonas fluorescens SBW25 (PFS)	Lab stock	Thompson et al.[84], Soil
Pedobacter heparinus (PH)	German Collection of Microorganisms and Cell Cultures, DSMZ	DSM 2366
Pseudomonas putida KT2440 (PP)	Lab stock	DSM 6125
Pseudomonas syringae pv. tomato DC 3000 (PSD)	Lab stock	N/A
Pseudomonas syringae subsp. syringae van Hall 1902 (PST)	German Collection of Microorganisms and Cell Cultures, DSMZ	DSM 50315
Rahnella victoriana (RV)	German Collection of Microorganisms and Cell Cultures, DSMZ	DSM 27397
Serratia entomophila (SE)	German Collection of Microorganisms and Cell Cultures, DSMZ	DSM 12358
Serratia ficaria (SF)	Lab stock	Provided by Department of Microbiology, University of Osnabrück

(*Continued on next page*)

Continued

REAGENT or RESOURCE	SOURCE	IDENTIFIER
Variovorax boronicumulans (VB)	This study	Soil isolate from sample site coordinates 50.906557, 11.505631
Recipients		
Acinetobacter baylyi ADP1, Δ*hisD::kanR*	Oña et al.[66]	N/A
Acinetobacter baylyi ADP1, Δ*trpB::kanR*	Oña et al.[66]	N/A
Escherichia coli BW25113, Δ*hisD::kanR*	Oña et al.[66]	N/A
Escherichia coli BW25113, Δ*trpB::kanR*	Oña et al.[66]	N/A
Software and algorithms		
Origin Pro 2017	OriginLab, Northampton, MA	https://www.originlab.com/index.aspx?go=Products/Origin
IBM SPSS statistics 26	IBM Corp. Released 2019. IBM SPSS Statistics, Version 26.0. Armonk, NY: IBM Corp	https://www.ibm.com/support/pages/downloading-ibm-spss-statistics-26
MEGA X	Kumar et al.[85]	https://www.megasoftware.net/
iTOL	Letunic and Bork[86]	https://itol.embl.de/
Softmax Pro 6 software	Molecular Devices	N/A
R version 3.5.3	R Development Core Team[87]	http://www.R-project.org
Mathematica	N/A	https://www.wolfram.com/mathematica/

RESOURCE AVAILABILITY

Lead contact

Further information and requests for resources should be directed to and will be fulfilled by the lead contact, Christian Kost (christiankost@gmail.com).

Materials availability

Strains generated and isolated in this study are available from the lead contact upon request.

Data and code availability

The datasets supporting the current study are available from the Lead Contact on request. This study did not generate any code.

EXPERIMENTAL MODEL AND SUBJECT DETAILS

Bacterial strains and their construction

Twenty-five bacterial wild-type strains were used as potential amino acid donors (key resources table). *Escherichia coli* BW25113 and *Acinetobacter baylyi* ADP1 were used as parental strains, from which mutants that are auxotrophic for histidine (Δ*hisD*) or tryptophan (Δ*trpB*) were generated. The gene to be deleted to create the corresponding auxotrophy was identified using the KEGG[88] and the EcoCyc[89] database. For *E. coli*, deletion alleles were transferred from existing single-gene deletion mutants (i.e., the Keio collection,[83]) into *E. coli* BW25113 using phage P1-mediated transduction.[90] In-frame knockout mutants were achieved by the replacement of target genes with a kanamycin resistance cassette. In the case of *A. baylyi*, deletion mutants were constructed as described previously.[36] Briefly, linear constructs of the kanamycin resistance cassette with 5′ overhangs homologous to the insertion site were amplified by PCR, where pKD4 was used as a template (see Table S2 for primer details). Upstream and downstream regions homologous to *hisD* and *trpB* were amplified using primers with a 5′-extension complementary to the primers used to amplify the kanamycin resistance cassette. The three amplified products (upstream, downstream, and kanamycin) were combined by PCR, resulting in overhanging flanks with a kanamycin cassette. This PCR product was introduced into the *A. baylyi* WT strain. For this, the natural competence of *A. baylyi* was harnessed. The transformation was done by diluting 20 μL of a 16 h-grown culture in 1 mL lysogeny broth (LB). This diluted culture was mixed with 50 μL of the above PCR mix and further incubated at 30°C with shaking at 200 rpm for 3 h. Lastly, 1 mL volume was pelleted, washed once with LB broth, plated on LB agar plates containing kanamycin (50 μg ml^{-1}), and incubated at 30°C for colonies to grow.

Conditional lethality of constructed auxotrophic mutations in MMAB medium was verified by inoculating 10^5 colony-forming units (CFU) ml^{-1} of these strains into 1 mL MMAB medium with or without the focal amino acid (100 μM). After 24 h, their optical density (OD) was determined spectrophotometrically at 600 nm using FilterMax F5 multi-mode microplate reader (Molecular Devices), and the mutation was considered conditionally essential when growth did not exceed the OD_{600nm} of the uninoculated minimal medium.[66,83,91]

Soil sampling, bacterial isolation, 16S rRNA gene amplification, and taxonomic affiliation

Soil samples were collected from a meadow site in Jena, Germany. A soil column of 50 mm diameter and 50 mm length was collected using a soil sampler and transported to the lab without disturbing its structure. The sample was processed by carefully dissecting the soil, and three 1 mg soil particles, which were spaced 2.5 cm apart, were selected for bacterial strain isolation. Soil particles were then suspended in 500 μl of saline solution (0.9% NaCl) and shaken for 30 mins. After that, 100 μl were transferred into 400 μl saline solution and vortexed vigorously for 5 min. Next, 100 μl of the previously prepared dilutions were spread on agar plates (in three replicates). The medium used for isolation was MMAB minimal medium with fructose as a sole carbon source and supplemented with all twenty biogenic amino acids (200 μM each), five different vitamins (i.e., riboflavin (B_2), cobalamin (B_{12}), biotin (B_7), thiamine (B_1), and pyridoxine (B_6), each at 1 μM). In addition, 100 μg ml^{-1} of the fungicide Nystatin was added to the media. Plates were incubated for three days at room temperature. After incubation, all colonies were picked and purified three times on agar plates to finally isolate a single colony. The resulting isolates were inoculated into 96-well plates containing the previously used medium and incubated under shaking conditions for 30 hours. Finally, glycerol was added to a final concentration of 50% (vol/vol) to prepare stocks that were frozen at −80°C until further use.

Five bacterial isolates (i.e., *Peribacillus simplex, Variovorax boronicumulans, Cupriavidus metallidurans, Bacillus licheniformis*, and *Nocardia coeliaca*) were characterized by reviving the focal strains and PCR-amplifying and sequencing part of the housekeeping 16S rRNA gene. For this, 1 μl of bacterial biomass from an overnight-grown culture was directly used as PCR template. The 16S rRNA gene was amplified using the general eubacterial primers FP and RP,[92] (Table S2) on a Biometra TProfessional Thermocycler (Biometra, Jena, Germany) in 20 μl reaction volumes using JumpStart REDTaq ReadyMix (Sigma Aldrich). 96-well plates were sealed with adhesive film. The following parameters were used: 3 min at 94°C, followed by 32 cycles of 40 s at 94°C, 60 s at 65°C and 60 s at 72°C, and a final extension step of 4 min at 72°C. PCR products were checked on an agarose gel, purified, treated with Shrimp alkaline phosphatase (Illustra, Fischer Scientific), and sequenced using an ABI 3730XL capillary DNA sequencer (Applied Biosystems, USA) in the Department of Entomology, Max-Planck-Institute for Chemical Ecology in Jena, Germany.

The forward and reverse 16S rRNA gene sequences were assembled and manually curated using Microsoft Word Office 2011 to generate contigs after trimming the poor sequences at both ends. Similarity-based searches were carried out using NCBI BLASTn[93] for taxonomic assignment of 16S rRNA gene sequences. The species of the five focal strains have been taxonomically identified based on sequence similarity to their nearest neighbor by using minimum query coverage of 98% and minimum identity values of 99%.

The 16S rRNA gene sequences of the 5 soil-derived strains used in this study have been deposited in GenBank under the following accession number, *Peribacillus simplex* (MW073531), *Variovorax boronicumulans* (MW073532), *Cupriavidus metallidurans* (MW073533), *Bacillus licheniformis* (MW073534), and *Nocardia coeliaca* (MW080346-MW080347).

METHOD DETAILS

Culture conditions and general procedures

A modified minimal media for Azospirillum brasilense (MMAB,[94]) was used for all experiments containing K_2HPO_4 (3 g L^{-1}), NaH_2PO_4 (1 g L^{-1}), KCl (0.15 g L^{-1}), NH_4Cl (1 g L^{-1}), $MgSO_4 \cdot 7H_2O$ (0.3 g L^{-1}), $CaCl_2 \cdot 2H_2O$ (0.01 g L^{-1}), $FeSO_4 \cdot 7H_2O$ (0.0025 g L^{-1}), $Na_2MoO_4 \cdot 2H_2O$ (0.05 g L^{-1}), and 5 g L^{-1} D-glucose as a carbon source. 10 mL of trace salt solution was added per liter of MMAB media from the 1L stock. Trace salt stock solution consisted of filter-sterilized 84 mg L^{-1} of $ZnSO_4$. $7H_2O$, 765 μl from 0.1 M stock of $CuCl_2$. $2H_2O$, 8.1 μl from 1 M stock of $MnCl_2$, 210 μl from 0.2 M stock of $CoCl_2$. $6H_2O$, 1.6 mL from 0.1 M stock of H_3BO_3, 1 mL from 15 gL^{-1} stock of $NiCl_2$.

All strains were precultured in replicates by picking single colonies from LB agar plates, transferring them into 1 mL of liquid MMAB in 96-deep well plate (Eppendorf, Germany) incubating these cultures for 20 h. In all experiments, auxotrophs were precultured at 30°C in MMAB, supplemented with 100 μM of the required amino acid. The next day, precultures were diluted to an optical density of 0.1 at 600 nm as determined by FilterMax F5 multi-mode microplate readers (Molecular Devices).

Coculture experiment

Approximately 50 μl of preculture were inoculated into 1 mL MMAB, leading to a starting density of 0.005 OD. In the case of cocultures, donor and recipient were mixed in a 1:1 ratio by co-inoculating 25 μl of each diluted preculture without amino acid supplementation. Monocultures of both donors and recipient (with and without the focal amino acid) were inoculated using 50 μl of preculture. Cultures were incubated at a temperature of 30°C and shaken at 220 rpm. Cell numbers were determined at 0 h and 24 h by serial dilution and plating. Donor strains were plated on MMAB agar plates, whereas recipients (auxotrophs) were differentiated on LB agar containing kanamycin (50 μg ml^{-1}) to select for recipient strains. For reagent and resources, see key resources table.

Relative fitness measurement

To quantify the effect of amino acid cross-feeding on the fitness of the recipient, the number of colony-forming units (CFU) per ml was calculated for monoculture and coculture conditions at 0 h and 24 h. Each donor was individually paired with one of the recipients as well as grown in monoculture. Every combination was replicated four times. The relative fitness of each recipient was determined by dividing the growth of each genotype achieved in coculture by the value of its respective monoculture. Since different donor genotypes showed inherent differences in growth (Figure 1C) and total amino acid production was negatively correlated with growth of

donors in monoculture (Spearman rank correlation: $\rho = -0.77$, $p = 8.8x\ 10^{-20}$, $n = 97$), growth of recipients in coculture was additionally normalized for donor growth. For this, growth of recipients in monoculture was first subtracted from its growth in coculture and then divided by the growth the respective donor genotype achieved under coculture conditions.

Amino acid supernatant experiment

To determine whether cross-feeding was mediated via compounds that have been released into the extracellular environment, the cell-free supernatants of donor genotypes were harvested and provided to receiver strains. To collect the supernatant, donors were grown in 2.5 mL MMAB in 48-deep well plates (Axygen, USA) and cultivated at 30°C under shaking conditions (220 rpm). Supernatants were isolated in the mid-exponential growth phase and centrifuged for 10 min at 4,000 rpm. Then, supernatants were filter-sterilized (0.22 μm membrane filter, Pall Acroprep, USA) and stored at −20°C. Meanwhile, receivers were grown in 1 mL MMAB in 96-well plates for 24 h. After adjusting the receiver OD_{600nm} to 0.1, 5 μl of the receiver culture was added to the replenished donor supernatant (total culturing volume: 200 μl, i.e., 160 μl donor supernatant + 40 μl MMAB) in 384-well plates (Greiner bio-one, Austria) (total: 50 μl culture). Four replicates of each comparison were grown for 24 h at 30°C in a FilterMax F5 multi-mode microplate reader (Molecular Devices). MMAB without supernatant and monocultures of receiver strains were used as control. Growth was determined by measuring the optical density at 600 nm every 30 minutes, with 12 minutes of orbital shaking between measurements. OD_{600nm} was measured and analyzed to calculate the maximum optical density (OD_{max}) achieved by the receiver strain using the Softmax Pro 6 software (key resources table). For each donor supernatant-receiver pair, OD_{max} achieved by receivers with supernatant was subtracted from the values achieved by cultures grown without supernatant and normalized with the OD_{600nm}, the respective donor strain had achieved at the time of supernatant extraction.

Amino acid quantification by LC-MS/MS

All 20 proteinogenic amino acids in the culture supernatant were analyzed. 100 μl of extracted supernatant was derivatised using the dansyl chloride method.[95,96] Norleucine was added as an internal standard to the sample, and a calibration curve was generated by analyzing all 20 amino acids at different concentrations. All samples were directly analyzed via LC-MS/MS. Chromatography was performed on a Shimadzu HPLC system. Separation was achieved on an Accucore RP-MS 150 × 2.1, 2,6 μm column (Thermo Scientific, Germany). Formic acid 0.1% in 100% water and 80% acetonitrile were employed as mobile phases A and B. The mobile phase flow rate was 0.4 mL min^{-1}, and the injection volume was 1 μl. Liquid chromatography was coupled to a triple-quadrupole mass spectrometer (ABSciex Q-trap 5500). Other parameters were: curtain gas: 40 psi, collision gas: high, ion spray voltage (IS): 2.5 keV, temperature: 550°C, ion source gas: 1: 60 psi, ion source gas 2: 70 psi. Multiple reaction monitoring was used to determine the identity of the focal analyte. Analyst and Multiquant software (AB Sciex) were used to extract and analyze the data.

Amino acid profile-based distance calculation using supernatant data

The similarity in the amino acid production profiles of different donor species was determined by calculating the Euclidean distance. If the amino acid production of a donor that is closely related to the focal auxotroph is given by $CR = (cr_1, cr_2, \cdots, cr_{20})$, and the amino acid production of a distantly related donor is given by $DR = (dr_1, dr_2, \cdots, dr_{20})$, the Euclidean distance between recipient and donor is:

$$ED(CR, DR) = \sqrt{(cr_1 - dr_1)^2 + (cr_2 - dr_2)^2 + \cdots + (cr_{20} - dr_{20})^2}$$

Index numbers (1-20) refer to individual amino acids.

Phylogenetic tree construction and distance calculation

To cover a broad taxonomic diversity of donor strains, we chose 25 well-characterized species, belonging to four different phyla. The 16S rRNA gene sequences of 20 strains were retrieved from the NCBI GenBank and 5 strains from 16S rRNA gene sequencing (STAR Methods). The phylogenetic tree of this marker gene was generated using the maximum likelihood method in MEGA X software.[85] 16S rRNA gene locus sequences of all strains were aligned with MUSCLE. Maximum-likelihood (ML) trees were constructed using the Kimura 2-parameter model, where rates and patterns among mutated sites were kept at uniform rates, yielding the best fit. Bootstrapping was carried out with 1,000 replicates. The phylogenetic tree was edited using the iTOL online tool (key resources table).[86] Pairwise phylogenetic distances between donor and receiver strains were extracted from a phylogenetic distance-based matrix. The resulting values quantify the evolutionary distance that separates the organisms.

Reconstruction of metabolic networks

Genome-scale metabolic networks for all organisms (key resources table) were reconstructed based on their genomic sequences using the gapseq software (version v0.9, https://github.com/jotech/gapseq).[97] In brief, the reconstruction process is divided into two main steps. First, reactions and pathway predictions, and second, gap-filling of the network to facilitate *in-silico* biomass production using flux balance analysis. For the reaction and pathway prediction step, all pathways from MetaCyc database[98] that are annotated for the taxonomic range of bacteria were considered. Of each reaction within pathways, the protein sequences of the corresponding enzymes were retrieved from the SwissProt database[99] and aligned against the organism's genome sequence by the TBLASTN algorithm.[100] An enzyme, and thus the corresponding reaction, was considered to be present in the organism's metabolic

network if the alignment's bitscore was ≥200 and the query coverage ≥75%. Reactions were considered to be existing, if more than 75% of the remaining reactions within the pathway were predicted to be present by the BLAST-searches or if more than 66% of the key enzymes, which are defined for each pathway by MetaCyc, were predicted to be part of the network by the blast searches. As reaction database for model construction, we used the ModelSEED database for metabolic modeling.[101]

The second step (i.e., the gap-filling algorithm of gapseq) solves several optimization problems by utilizing a minimum number of reactions from the ModelSEED database and adding them to the network to facilitate growth in a given growth medium. Here, the chemical composition of the M9 medium (which is qualitatively identical to MMAB) with glucose as sole carbon source was assumed.

The genome sequences for the 25 strains used in this study's experiments (key resources table) were retrieved from the genome assembly database from NCBI Refseq. For 19 out of the 25 strains, genome assemblies for the same strains were available from NCBI Refseq. For the remaining six strains (*S. entomophila, N. coeliaca, B. simplex, C. metallidurans, B. licheniformis, V. boronicumulans*) an assembly of a closely related strains was identified by using NCBI's BLASTN algorithm to align the strains' sequenced 16S rRNA gene sequence (see method) against all available bacterial genome assemblies in Refseq. A complete list of the strain-assembly-mapping is provided in the Table S3. The genome-scale metabolic models of the 818 human gut microorganisms were reconstructed on the basis of genomes provided by the Virtual Metabolic Human (VMH) online platform (https://www.vmh.life/#microbes/search).

Calculating the genome-based metabolic distance of organisms

To estimate the pairwise metabolic distance between donor and recipient genotypes, the structure of their metabolic network was compared. For this, a flux balance analysis was performed on each individual metabolic network model with the biomass reaction flux as objective function. Subsequently, the biomass reaction flux was fixed to predicted maximum flux, and a second flux balance analysis was performed to minimize the sum of absolute fluxes throughout the entire network.[102] Pairwise distances of flux distributions between organisms were calculated as the Euclidean distance between the predicted flux vectors. Only reactions with a non-zero flux in at least one of the two organisms were included in the distance approximations. In case a reaction was absent in one of the models, the flux was considered zero.

In silico simulation of bacterial co-growth

To further investigate the relationship between the metabolic distance between organisms and the likelihood of entering into a cross-feeding interaction, we extended our analysis to a larger number of bacterial organisms using *in silico* co-growth simulations. For this, we reconstructed 818 bacterial metabolic network models as described above. The selected 818 organisms are the same as from the AGORA-collection, representing common members of the human gut microbiota.[103] For co-growth simulations, the models were merged in a pairwise manner, as described previously.[104,105] The predicted flux values of the two individual biomass reactions (i.e., growth rate) were compared to the predicted growth rates of the respective models in monoculture, which enabled the prediction of potential growth benefits from metabolic interactions between both species. If at least one of two models was predicted to have a 20% higher growth rate in coculture than in monoculture, the pair was considered as an interaction pair with growth advantage (Figure 4). A logistic curve function of the form $y = a/(1 + Exp[-b (x - c)])$ was fitted to the data.

QUANTIFICATION AND STATISTICAL ANALYSIS

Normal distribution of data was evaluated employing the Kolmogorov-Smirnov test, and data was considered to be normally distributed when $p > 0.05$. Homogeneity of variance was determined using Levene's test, and variances were considered homogeneous if $p > 0.05$. Differences in recipient growth in coculture versus monocultures were assessed with paired sample t tests. P values were corrected for multiple testing by applying the false discovery rate (FDR) procedure of Benjamini et al.[106,107] Linear regressions were used to assess the growth support of recipients in cocultures as a function of different variables (i.e., amino acid profile distance, phylogenetic distances, and metabolic distance). Spearman's rank correlation was used to assess the relationship between amino acid production and growth of recipient as maximum density when cultured with donor supernatants. The relationship between each proxy tested and recipient growth was depicted as a 2D plane and analyzed by fitting a linear regression. Regression analyses was also used to disentangle the effect of more than one interacting predictor variable. In these cases, the phylogenetic signal or amino acid produced was controlled for the respective other predictor variable (e.g., metabolic distance or amino acid production profile distance) used to predict the growth of recipient. To rule out collinearity between variables, the variance inflated factor (VIF) was calculated for all potential pairs of variables that have been used to predict growth. In all cases, VIF values were well below the critical threshold (VIF = 5),[108] thus suggesting no multicollinearity.